

## ORIGINAL RESEARCH ARTICLE

## Diagnostic accuracy of multiparametric magnetic resonance imaging for pelvic lymph node metastasis in prostate cancer

Hardi Shwan Mahialdin<sup>1\*</sup> and Hana Rizgar Muhammed Ameen<sup>2</sup><sup>1</sup>Department of Urology, Ashti Teaching Hospital, Soran/Erbil, Kurdistan Region of Iraq<sup>2</sup>Oncology Department, Rizgary Teaching Hospital, Erbil, Kurdistan Region of Iraq

## Abstract

Prostate cancer (PCa) is the second most common cancer in men, and can be detected through various modalities. Magnetic resonance imaging (MRI) is a good imaging modality for PCa detection, localization, and staging. This study evaluates the role of multiparametric MRI in detecting lymph node metastasis in PCa patients. A prospective study was conducted at Erbil urology center/in Iraq, targeting patients planning to have a radical prostatectomy with pelvic lymphadenectomy between April 2022 and December 2022. This study included 30 patients diagnosed with PCa; every patient underwent both preoperative MRI of the prostate and radical prostatectomy with extended pelvic lymph node dissection. MRI findings and histopathology results were compared for accuracy. Nodal metastasis was detected in 6/30 (20%) of cases. Overall, 6/30 (20%) had enlarged pelvic lymph nodes shown on MRI. Enlarged internal iliac lymph nodes were most common, found in 4/6 (66.7%) patients. There was a slight agreement between MRI T-stage and pathological T-stage (Kappa= 0.179,  $p=0.08$ ). Lymph node enlargement on MRI showed moderate accuracy (area under the curve [AUC] = 0.708), with sensitivity and positive predictive value of 66.7% and specificity and negative predictive value of 91.7%. Although the predictor was significantly associated with lymph node metastasis (log-odds ratio = 0.012,  $p = 0.01$ ), its ability to distinguish patients with nodal involvement from those without was moderate (AUC = 0.708). This study suggests that preoperative MRI parameters, when combined with clinical features, may have limited value in predicting nodal metastases.

**\*Corresponding author:**  
Hardi Shwan Mahialdin  
(dr.hardishwan@gmail.com)

**Citation:** Mahialdin HS, Muhammed Ameen HR. Diagnostic accuracy of multiparametric magnetic resonance imaging for pelvic lymph node metastasis in prostate cancer. *Cancer Plus*. 2026;8(2):025440067. doi: 10.36922/CP025440067

**Received:** October 27, 2025

**Revised:** April 30, 2026

**Accepted:** May 13, 2026

**Published online:** June 23, 2026

**Copyright:** © 2026 Author(s). This is an Open-Access article distributed under the terms of the Creative Commons Attribution License, permitting distribution, and reproduction in any medium, provided the original work is properly cited.

**Publisher's Note:** AccScience Publishing remains neutral with regard to jurisdictional claims in published maps and institutional affiliations.

**Keywords:** Prostate-specific antigen; Prostate cancer; Extended pelvic lymph node dissection

## 1. Introduction

After lung cancer, prostate cancer is the second most prevalent disease diagnosed in males worldwide. It is also the fifth leading cause of cancer-related deaths in men.<sup>1</sup> Acinar adenocarcinomas account for 90–95% of prostate cancers.<sup>1</sup> Most of the other instances are attributed to neuroendocrine and ductal carcinoma. Prostate tumors, including subtypes of acinar adenocarcinoma, are listed in detail in the 2016 World Health Organization classification.<sup>2</sup> As men age, the incidence of prostate cancer

increases; up to 60% of men over 65 may receive a prostate cancer diagnosis, with an average age of 66 at diagnosis.<sup>3</sup>

Ethnicity, age, and place of residence are known risk factors for prostate cancer.<sup>4</sup> Research on age-specific incidence curves shows that the risk of prostate cancer increases significantly after the age of 55, peaks between the ages of 70 and 74, and then gradually declines after that. According to autopsy reports, many men have early-stage prostate cancer lesions in their 20s and 30s, and the disease has a lengthy induction period.<sup>5</sup>

Genetic susceptibility and family history are additional risk factors. Men who have a family history of breast cancer (one or more first-degree relatives) are 21% more likely to be diagnosed with prostate cancer and 34% more likely to die from the disease than men without such a history. Similarly, there is a general trend that favors increases in risk based on earlier cancer initiation in families; a family history of prostate cancer increases risk by 68% and lethality of the illness by 72%.<sup>4</sup> Prostate cancer incidence and/or mortality have also shown varying relationships with dietary components, activity, nutritional supplementation and/or deficiency, and smoking.<sup>6</sup>

Several methods are available for detecting prostate cancer in men. In certain nations, prostate-specific antigen (PSA) is widely used as a prostate cancer screening test, which has increased the number of asymptomatic men receiving a diagnosis. Men are examined for prostate cancer when they complain of lower urinary tract symptoms or other genitourinary symptoms. According to autopsy studies, up to three-quarters of men over 85 had neoplastic changes in their prostates, though not all of them had been diagnosed prior to their death. This suggests that a sizable portion of men pass away from prostate cancer without receiving a diagnosis.<sup>7</sup>

Magnetic resonance imaging (MRI) is an effective imaging modality for prostate cancer detection, localization, and staging.<sup>8</sup> False-positive results, including prostatitis, post-biopsy bleeding, and fibrosis, may affect how prostate cancer is interpreted on T2-weighted MRI.<sup>9</sup> Functional MRI techniques, including diffusion-weighted MRI<sup>10</sup>, proton MR spectroscopic imaging<sup>11</sup>, and dynamic contrast-enhanced MRI, have been used to increase the diagnostic accuracy of prostate cancer imaging.<sup>12</sup>

Over time, it has been shown that the Gleason prostate cancer score is the most accurate and predictive histological grading system currently in use. Originally created in the 1960s by pathologist Dr. Donald Gleason, it is now used for all pathological descriptions of prostate cancer.<sup>13</sup>

Based on clinical experience with the previous Gleason scoring system, the World Health Organization proposed

a new categorization system in 2016. It suggested that patients with lower Gleason scores had little variation in clinical outcomes, whereas those with higher grades showed greater variation.<sup>14</sup>

The most promising treatment for localized prostate cancer is radical prostatectomy, which also significantly improves overall survival, cancer-specific survival, and the occurrence of distant metastases. These advantages over other conclusive, curative treatments are especially significant in males under 65 at the time of diagnosis and do not become apparent 10 years after therapy for localized disease. If there are distant metastases or the tumor is attached to nearby structures, radical prostatectomy is not a suitable treatment.<sup>15</sup>

The effect of lymph node involvement varies depending on the degree of nodal disease, although it is a significant prognostic factor in prostate cancer. According to earlier research, patients with lymph node metastases have poorer cancer-specific survival rates than node-negative patients, with 5- and 10-year survival rates of roughly 94% and 83%, respectively.<sup>16</sup> The significance of nodal burden is further demonstrated by long-term results in individuals with lymph node-positive prostate cancer. An overall median survival of almost 15 years has been reported in studies with extended follow-up (median 11.4 years), with recurrence-free survival rates of 80%, 65%, and 58% at 5, 10, and 15 years, respectively. Significantly better results were observed in patients with minor nodal involvement (1–2 positive lymph nodes) than in those with extensive nodal disease, with 10-year recurrence-free survival rates of approximately 70% compared to 49% in patients with  $\geq 5$  affected nodes. Furthermore, a significantly higher risk of recurrence was associated with lymph node density  $\geq 20\%$ , highlighting the importance of both the quantity and percentage of affected lymph nodes as prognostic factors.<sup>17</sup>

Although histopathological evaluation following pelvic lymph node dissection (PLND) remains the current gold standard for lymph node staging in prostate cancer, it has several important limitations. PLND is an invasive procedure associated with perioperative complications and additional patient morbidity.<sup>18</sup> Moreover, due to the complex and highly variable lymphatic drainage of the prostate, accurate staging requires the removal of a large number of lymph nodes, and there is still no consensus regarding the optimal anatomical extent of dissection.<sup>18</sup> Even with extended PLND, a substantial proportion of metastatic lymph nodes may be missed, as up to one-third of metastases can lie outside the standard dissection template.<sup>19</sup> In addition, histopathological assessment may underestimate disease burden, detecting fewer metastatic nodes compared to more sensitive molecular techniques.<sup>19</sup>

Furthermore, PLND has been shown to underestimate lymph node involvement, with studies reporting that 40–50% of metastatic nodes may be located outside routine resection areas and that even extended dissection can miss approximately 13% of metastatic nodes.<sup>20</sup> These limitations highlight that histopathology may not fully reflect the true extent of nodal disease and emphasize the need for more accurate, non-invasive diagnostic approaches.

Even with current advancements, it is still very difficult to accurately detect lymph node metastases in prostate cancer prior to surgery. Due to sampling and anatomical constraints, histological evaluation may underestimate real nodal involvement, whereas conventional imaging methods have poor sensitivity. Consequently, more research is required to assess the diagnostic efficacy of MRI measures and their potential contribution to improved preoperative prediction of lymph node metastasis.

This study uses histopathology after extended PLND as the reference standard to assess the diagnostic accuracy of multiparametric MRI parameters in identifying metastatic pelvic lymph nodes in prostate cancer.

## 2. Methodology

### 2.1. Patient recruitment and data collection

This prospective study was conducted at the Erbil Urology Center in Iraq, including patients scheduled to undergo radical prostatectomy and pelvic lymphadenectomy between April 2022 and December 2022. A total of 30 patients with prostate cancer participated in this study; all underwent radical prostatectomy with extensive PLND and preoperative prostate MRI. Clinical variables evaluated included age at surgery, PSA density, ultrasound-derived prostatic volume, serum PSA level, and biopsy Gleason score.

Complete data on the total number of examined lymph nodes, the number of pathological lymph nodes, and the pathological stage and grade were collected. The finding of nodal metastasis on final histological examination was used as the standard reference. The data obtained from MRI imaging included: (i) MRI T-stage: according to the National Comprehensive Cancer Network guideline (version 1.2022), (ii) the tumor's location, and (iii) the number and location of the enlarged lymph nodes at MRI.

### 2.2. Magnetic resonance imaging

Prostate MRIs were performed on patients between weeks 3 and 5 after transrectal ultrasound-guided biopsies and before surgery. A 1.5T magnetic resonance imaging device (MR B17 syngo, A Tim system, Siemens Magnetom Avanto, Siemens Healthineers, Germany) was used to scan

the participants. A gadolinium-based contrast agent (0.5 mmol/mL; 279 mg/mL injection solution) was administered using a Medrad Spectris Solaris EP injector (Bayer, United States). The MRI examination included T1-weighted, T2-weighted, diffusion-weighted, and dynamic contrast-enhanced imaging. MRI examinations were interpreted by two experienced radiologists as part of routine clinical practice. The final radiology report, reflecting the agreed interpretation, was used for analysis. Both were blinded to the patients' clinical and histopathological information.

Lymph nodes were considered enlarged based on a short-axis diameter of  $\geq 8$  mm. In addition to size, morphological features such as round shape and irregular borders were also considered suggestive of possible malignancy. However, standardized scoring systems such as the Prostate Imaging Reporting and Data System were not applied for lymph node assessment. The MRI protocol is summarized in [Table 1](#).

### 2.3. Preoperative assessment and histopathology

Preoperative assessment included (i) laboratory assessments for basic metabolic panel, complete blood count, and prothrombin time/international normalized ratio; (ii) chest X-ray or computer tomography scan of the chest and cardiac evaluation, including electrocardiography and echocardiography; (iii) bone scan if there were related symptoms: PSA above 10 ng/mL and Gleason score  $\geq 7$ ; and (iv) blood preparation.

All patients underwent radical prostatectomy with extended PLND following standard surgical protocols. The resected tissues were sent for histopathological study, along with each side of the resected lymph nodes separately, for staging and grading of the tumor, lymph node involvement, and the pathological Gleason score. The histopathologist was completely blinded to the patients' MRI findings. Comparisons were made between patients without lymph node metastasis (pN0) and those with lymph node metastasis (pN1).

### 2.4. Ethical considerations

All patients received adequate information regarding the study aims and methods. Informed consent was obtained after discussing the surgical procedure, indications, potential risks and complications.

### 2.5. Statistical analysis

In descriptive statistics, frequencies and proportions were reported for categorical variables, and means, medians, and interquartile ranges (IQRs) for continuous variables. Continuous variables were compared using the independent samples *t*-test or the Mann–Whitney *U* test, depending on

Table 1. Magnetic resonance imaging protocols

| Parameter                       | T1-weighted MRI | T2-weighted MRI | DWI <sup>a</sup> | DCE-MRI   |
|---------------------------------|-----------------|-----------------|------------------|-----------|
| Orientation                     | Axial           | Axial           | Axial            | Axial     |
| TR/TE                           | 500/11          | 4,000/103       | 3,700/80         | 4.79/1.69 |
| Flip angle (°)                  | 150             | 150             | -                | 2.0       |
| Matrix                          | 256 × 75        | 320 × 80        | 160 × 70         | 142 × 192 |
| No. of excitation (Images/slab) | 20              | 20              | 20               | 20        |
| FOV (mm)                        | 200             | 200             | 260              | 260       |
| Slice thickness (mm)            | 3.0             | 3.0             | 3.0              | 3.6       |

Note: <sup>a</sup>Three different weighting factors (b values; 0,100, and 800) were used.

Abbreviations: DCE-MRI: Dynamic contrast-enhanced magnetic resonance imaging; DWI: Diffusion-weighted imaging; FOV: Field of view; MRI: Magnetic resonance imaging; TE: Echo time; TR: Repetition time.

the distribution of the data. To investigate the relationship between preoperative parameters and nodal invasion, univariate logistic regression analyses were performed. To determine the continuous variable's cutoff point with the maximum sensitivity and specificity, receiver operating characteristic (ROC) curves were constructed. The fitted logarithm of the odds ratio (logOR) was used to measure the correlation between the factors and the outcome. The Statistical Package for Social Sciences software (version 23) was used to conduct all statistical analyses. Due to the limited sample size, Fisher's exact test was used. A *p*-value < 0.05 was considered statistically significant.

### 3. Results

Thirty male patients were recruited prospectively for this study. The mean age of the patients was  $67.5 \pm 7.6$  years. The mean age of patients with pathological nodal metastasis was  $66.5 \pm 10.2$  years, and for patients without nodal metastasis it was  $67.6 \pm 7.1$  years.

Nodal metastasis was detected in 6/30 (20%) of cases, with a mean of 0.3 metastatic lymph nodes (range: 1–2). There was no significant difference in terms of mean age, serum PSA levels, prostate volume, and PSA density between the two groups of men, i.e., those who had and those who did not have nodal metastasis in terms of mean age (all *p* > 0.05). They also did not differ significantly in any other pathological or radiological parameters. Clinical, pathological, and radiological characteristics are shown in Tables 2 and 3.

Among patients with pathologic lymph node metastasis, 83.3% were  $\geq T2$  on MRI, and 16.7% were  $< T2$  (Table 3). However, according to the pathologic T-stage, 5/6 (83.3%) of patients with pathologic lymph nodes were in stage T3b, and 1/6 (16.7%) were in stage T4 (Table 2). Among patients with pathologic nodal metastasis, 66.7% had preoperative MRI-suspected pathological lymph nodes. The mean pathological grade was 3.43, as shown in Table 2.

Overall, 6/30 (20%) had enlarged pelvic lymph nodes shown on MRI. Enlarged internal iliac lymph nodes were most commonly found in 4/6 (66.7%) of patients. Only 1/6 (16.7%) of patients had enlarged periprostatic lymph nodes, and 1/6 (16.7%) had enlarged external iliac lymph nodes. There was slight agreement between MRI T-stage and pathological T-stage (Kappa = 0.179, *p* = 0.08).

Receiver operating characteristic curve analysis, illustrated in Figure 1, was used to evaluate the ability of serum PSA, prostatic volume, and PSA density to predict pathological lymph node involvement. The areas under the ROC curves (AUCs) were 0.743, 0.674, and 0.635, respectively, indicating modest discriminatory ability; serum PSA, prostatic volume, and PSA density perform better than chance but are not strong standalone predictors. A cut-off value of 12.6 ng/mL for serum PSA, 64.9 mL for prostatic volume, and 0.371 ng/mL/cc for PSA density was identified as the optimal threshold for predicting pathological lymph node positivity. At a 0.371 ng/mL/cc cut-off value for PSA density, the sensitivity was 66.7%, indicating that approximately two-thirds of patients

Table 2. Demographic, clinical, and histopathological characteristics of the patients

| Parameters                        | Overall (n = 30) | pN0 (n = 24)  | pN1 (n = 6)   | p-value            |
|-----------------------------------|------------------|---------------|---------------|--------------------|
| Age (years)                       |                  |               |               |                    |
| Mean (Median)                     | 67.5 (66.5)      | 67.6 (67.5)   | 66.5 (62.5)   | 0.204              |
| IQR                               | 13.5             | 13.3          | 12.3          |                    |
| PSA level (ng/mL)                 |                  |               |               |                    |
| Mean (Median)                     | 22.6 (20.5)      | 19.2 (20.1)   | 36.6 (31.3)   | 0.073 <sup>a</sup> |
| IQR                               | 21.7             | 19.6          | 14.9          |                    |
| Prostatic volume by US (mL)       |                  |               |               |                    |
| Mean (Median)                     | 56.6 (38.6)      | 54 (38.1)     | 67.2 (70.1)   | 0.195 <sup>a</sup> |
| IQR                               | 34.4             | 35.9          | 45.8          |                    |
| PSA density (ng/mL/cc)            |                  |               |               |                    |
| Mean (Median)                     | 0.486 (0.397)    | 0.456 (0.375) | 0.603 (0.622) | 0.312 <sup>a</sup> |
| IQR                               | 0.56             | 0.53          | 0.58          |                    |
| Biopsy Gleason score (%)          |                  |               |               |                    |
| 6                                 | 3 (10%)          | 3 (12.5%)     | 0 (0.0)       | 0.949              |
| 7                                 | 21 (70%)         | 18 (75%)      | 3 (50%)       |                    |
| 8–10                              | 6 (20%)          | 3 (12.5%)     | 3 (50%)       |                    |
| Pathologic T-stage                |                  |               |               |                    |
| pT1c                              | 2 (6.7%)         | 2 (8.3%)      | 0 (0.0)       | 0.111              |
| pT2                               | 3 (10%)          | 3 (12.5%)     | 0 (0.0)       |                    |
| pT2a                              | 1 (3.3%)         | 1 (4.2%)      | 0 (0.0)       |                    |
| pT2b                              | 2 (6.7%)         | 2 (8.3%)      | 0 (0.0)       |                    |
| pT2c                              | 9 (30%)          | 9 (37.5%)     | 0 (0.0)       |                    |
| pT3                               | 1 (3.3%)         | 1 (4.2%)      | 0 (0.0)       |                    |
| pT3a                              | 1 (3.3%)         | 1 (4.2%)      | 0 (0.0)       |                    |
| pT3b                              | 9 (30%)          | 4 (16.7%)     | 5 (83.3%)     |                    |
| pT4                               | 2 (6.7%)         | 1 (4.2%)      | 1 (16.7%)     |                    |
| Pathological grade, mean (median) | 3.43 (4)         | 3.46 (4)      | 3.33 (4)      | 0.784              |
| Pathologic Gleason score          |                  |               |               |                    |
| 6                                 | 3 (10%)          | 3 (12.5%)     | 0 (0.0)       | 0.411              |
| 7                                 | 13 (43.3%)       | 11 (45.8%)    | 2 (33.3%)     |                    |
| 8–9                               | 14 (46.7%)       | 10 (41.7%)    | 4 (66.7%)     |                    |
| No. of examined lymph nodes       |                  |               |               |                    |
| Mean (Median)                     | 12.9 (10)        | 13.63 (13)    | 10.33 (9)     | 0.947              |
| IQR                               | 8                | 8             | 11            |                    |
| No. of pathologic lymph nodes     |                  |               |               |                    |
| Mean                              | -                | -             | 1.5 (1.5)     | -                  |
| IQR                               | -                | -             | 2             |                    |

Notes: Percentages refer to the total number of the corresponding population (overall, pN0, or pN1). pN0 stands for the absence of lymph node metastasis at pathologic examination. pN1 indicates the presence of nodal metastasis on pathologic examination. <sup>a</sup>Calculated using the Mann–Whitney *U* test.

Abbreviations: IQR: Interquartile range; PSA: Prostate-specific antigen; US: Ultrasound.

Table 3. Radiological characteristics of the patients

| Parameters                            | Overall ( <i>n</i> = 30) | N0 ( <i>n</i> = 24) | N1 ( <i>n</i> = 6) | <i>p</i> -value |
|---------------------------------------|--------------------------|---------------------|--------------------|-----------------|
| Location on MRI                       |                          |                     |                    |                 |
| PZ                                    | 20 (66.7%)               | 15 (62.5%)          | 5 (83.3%)          | 1.00            |
| TZ                                    | 3 (10%)                  | 3 (12.5%)           | 0 (0.0)            |                 |
| CZ                                    | 1 (3.3%)                 | 1 (4.2%)            | 0 (0.0)            |                 |
| PZ+TZ                                 | 6 (20%)                  | 5 (20.8%)           | 1 (16.7%)          |                 |
| MRI T-stage                           |                          |                     |                    |                 |
| mT1                                   | 2 (6.7%)                 | 1 (4.2%)            | 1 (16.7%)          | 0.427           |
| mT1b                                  | 1 (3.3%)                 | 1 (4.2%)            | 0 (0.0)            |                 |
| mT2                                   | 11 (36.7%)               | 10 (41.7%)          | 1 (16.7%)          |                 |
| mT2a                                  | 1 (3.3%)                 | 1 (4.2%)            | 0 (0.0)            |                 |
| mT2b                                  | 2 (6.7%)                 | 2 (8.3%)            | 0 (0.0)            |                 |
| mT2c                                  | 5 (16.7%)                | 4 (16.7%)           | 1 (16.7%)          |                 |
| mT3                                   | 5 (16.7%)                | 4 (16.7%)           | 1 (16.7%)          |                 |
| mT3a                                  | 1 (3.3%)                 | 0 (0.0)             | 1 (16.7%)          |                 |
| mT3b                                  | -                        | -                   | -                  |                 |
| mT4                                   | 2 (6.7%)                 | 1 (4.2%)            | 1 (16.7%)          |                 |
| Lymph node involvement (%)            |                          |                     |                    |                 |
| Patients with enlarged lymph nodes    | 6 (20%)                  | 2 (8.3%)            | 4 (66.7%)          | 0.007           |
| Patients with no enlarged lymph nodes | 24 (80%)                 | 22 (91.7%)          | 2 (33.3%)          |                 |

Notes: Percentages refer to the total number of the corresponding population (overall, pN0, or pN1). pN0 stands for the absence of lymph node metastasis at histopathologic examination. pN1 denotes the presence of nodal metastasis on histopathologic examination. *p*-value was calculated by Fisher's exact test, and it indicates the difference between the pN0 and pN1 groups.

Abbreviations: CZ: Central zone; LN: Lymph node; MRI: Magnetic resonance imaging; PZ: Peripheral zone; TZ: Transitional zone.

with pathological lymph node involvement were correctly identified, while the specificity was 50%. This reflects a balanced but limited trade-off between sensitivity and specificity, suggesting that PSA density may be useful as an adjunctive marker rather than a definitive diagnostic tool.

Univariate logistic regression analysis and performance characteristics of preoperative variables are shown in Table 4. Biopsy Gleason score was significantly associated with nodal metastasis on final histopathology ( $p < 0.05$ ), with the highest accuracy (AUC = 0.896), a sensitivity and

positive predictive value of 50%, and a specificity and negative predictive value of 87.5%. Biopsy Gleason Score is a good predictor of lymph node metastasis (LogOR = 13.4,  $p$ -value = 0.03) when the patient has a score > 7. Meanwhile, lymph node enlargement on MRI showed sensitivity and positive predictive value of 66.7% and specificity and negative predictive value of 91.7%. Moreover, although the predictor showed a statistically significant association with lymph node metastasis (LogOR = 0.012,  $p = 0.01$ ), its discriminative performance was moderate (AUC = 0.708), indicating limited ability to distinguish patients with from

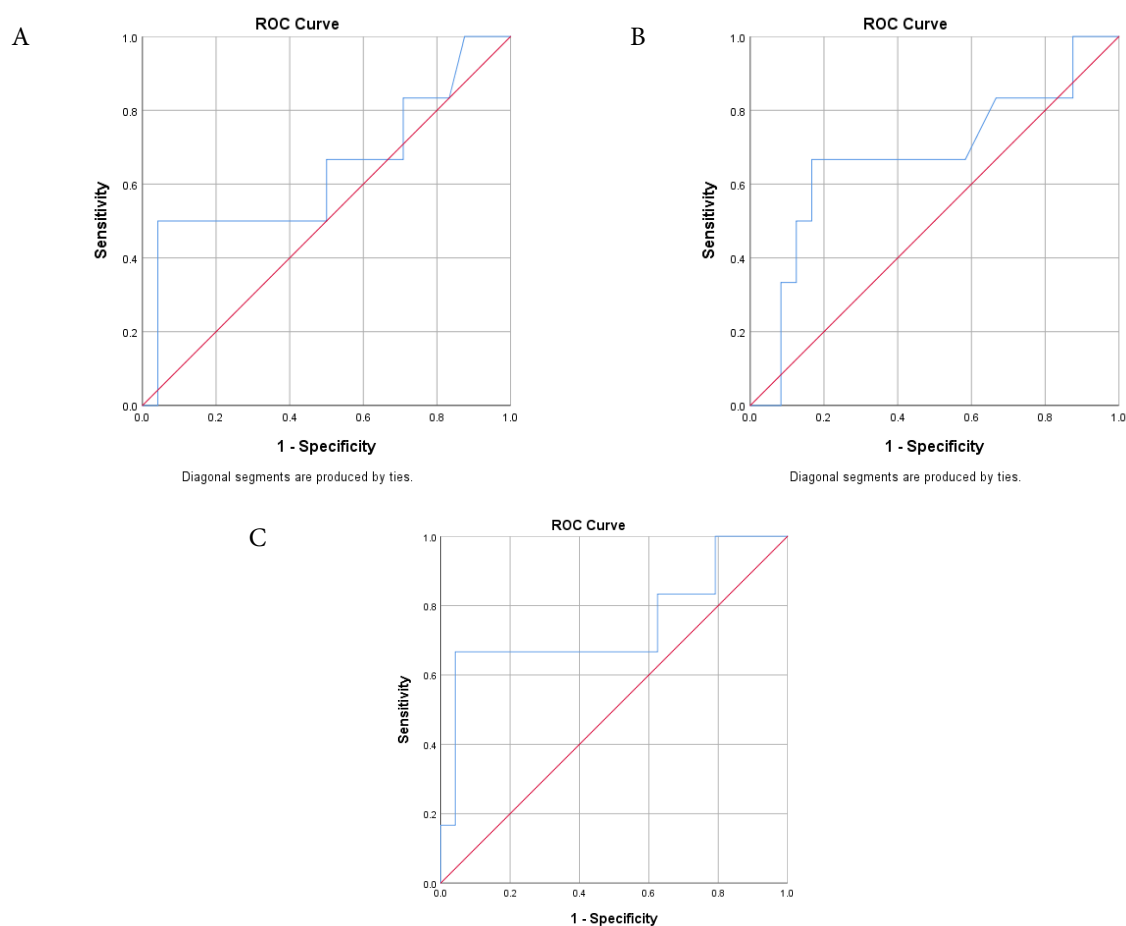


**Figure 1.** Receiver operating characteristic curves. (A) Prostate-specific antigen (PSA) density, (B) prostatic volume, and (C) serum PSA for predicting pathological lymph nodes.

**Table 4. Univariate logistic analysis and diagnostic performance analyses**

| Parameter            | Threshold | Sens % | Spec % | PPV % | NPV % | AUC   | LogOR | <i>p</i> -value |
|----------------------|-----------|--------|--------|-------|-------|-------|-------|-----------------|
| PSA (ng/mL)          | 12.6      | 83.3   | 37.5   | 25    | 90    | 0.743 | 0.912 | 0.227           |
| Biopsy Gleason score | >7        | 50     | 87.5   | 50    | 87.5  | 0.896 | 13.4  | 0.03            |
| MRI T-stage          | ≥T2       | 83.3   | 8.3    | 18.5  | 66.7  | 0.458 | 0.455 | 0.501           |
| Prostatic volume     | 64.9      | 66.7   | 83.3   | 50    | 91    | 0.624 | 1.006 | 0.748           |
| PSA density          | 0.371     | 66.7   | 50     | 25    | 85    | 0.635 | 11.6  | 0.462           |
| Enlarged LN          | +         | 66.7   | 91.7   | 66.7  | 91.7  | 0.708 | 0.012 | 0.01            |

Abbreviations: AUC: Area under the curve; LN: Lymph node; LogOR: Log odds ratio; MRI: Magnetic resonance imaging; NPV: Negative predictive value; PPV: Positive predictive value; PSA: Prostate-specific antigen; Sens: Sensitivity; Spec: Specificity.



those without nodal involvement. Note that pathologic lymph node positivity (pN1) was coded as the event of interest for ROC analysis

The prevalence of lymph node metastasis in relation to lymph node enlargement and PSA density is shown in Table 5. Preoperative PSA density combined with MRI findings of nodal enlargement showed that the prevalence of patients with LN metastasis among those with enlarged lymph nodes and PSA density > 0.371 ng/mL/cc was 3/5 (60%). The prevalence of lymph node metastasis among patients with enlarged lymph nodes and a PSA density < 0.371 was 1/13 (7.7%), and this association was statistically significant ( $p < 0.05$ )

#### 4. Discussion

In previous studies, as well as National Comprehensive Cancer Network clinical practice guidelines in oncology, CT and MRI are not advised for preoperative N-staging in males with prostate cancer due to their low sensitivity.<sup>21,22,23</sup> The preoperative likelihood of lymph node metastases should be considered when deciding whether to undergo a nodal dissection.<sup>17</sup> Preoperative nomograms, currently based solely on clinical parameters, can be used to estimate individual risk of lymph node metastasis.<sup>23,24,25</sup> However, preoperative MRI imaging techniques of the prostate may offer further insight into a number of prostatic tumor features linked to lymph node metastases. Prostate MRI, in particular, is the preferred imaging technique for local staging before surgery and, when paired with clinical data, enhances the prediction of the diseased T-stage.<sup>22</sup> This is crucial in this situation, as nodal metastasis rates are higher when the tumor stage is higher at the time of histopathologic testing.<sup>26</sup> In our study, MRI T-stage showed poor predictive performance for lymph node

metastases (AUC = 0.458), and the prevalence of nodal metastases was not significantly higher in patients with  $\geq T2$  tumors than in those with  $< T2$  tumors (18.5% [ $\geq T2$ ] vs. 33.3% [ $< T2$ ];  $p = 0.501$ ). This finding differs from Brembilla *et al.*<sup>27</sup>, in which they found that patients with T3 tumor stage had a significantly higher prevalence of nodal metastasis than those with T2 tumor stage. Their study showed that 57.1% of patients with T3 tumors had lymph node metastasis, whereas only 4.5% of their patients with T2 tumors had nodal invasion. The biopsy Gleason score showed the highest discriminative performance among the evaluated variables (AUC = 0.896,  $p = 0.03$ ); however, this finding should be interpreted with caution due to the small sample size. Although this finding is not consistent with Brembilla *et al.*<sup>27</sup>, several other studies<sup>23</sup> confirm that prostate needle biopsy is an important predictor of lymph node invasion. In detecting lymph node metastasis, MRI-detected lymph node enlargement had a sensitivity of 66.7% and a specificity of 91.7%. This finding is in line with previous studies<sup>28</sup>, in which sensitivity was significantly lower than specificity (14–36% and 91–97%, respectively); however, in our study, sensitivity was higher. Lymph node enlargement on MRI showed high specificity, and its overall discriminative performance was moderate (AUC = 0.708), indicating limited utility as a standalone predictor

In the current study, MRI-based T-staging showed slight agreement with histopathology results (Kappa = 0.179). An enlarged pelvic lymph node was found in 20% of our patients. This finding is higher than that reported by Brembilla *et al.*<sup>27</sup>, in which only 5.9% of patients had enlarged lymph nodes on MRI. Furthermore, 66.7% of our patients with nodal metastasis had MRI findings suggestive of lymph node involvement, based on enlarged lymph nodes. This rate was higher than that reported by Brembilla *et al.*<sup>27</sup>, who found suspicious enlarged lymph

**Table 5. Prevalence of lymph node metastasis according to nodal enlargement and prostate-specific antigen density**

| Groups  | LN metastasis on histopathologic examination | <i>p</i> -value |
|---|--|-----------------|
| Enlarged LN and PSA density < 0.371 ng/mL/cc    | 1/13 (7.7%)                                  | 0.011*          |
| Enlarged LN and PSA density > 0.371 ng/mL/cc    | 3/5 (60%)                                    |                 |
| No enlarged LN and PSA density < 0.371 ng/mL/cc | 1/1 (100%)                                   |                 |
| No enlarged LN and PSA density > 0.371 ng/mL/cc | 1/11 (9.1%)                                  |                 |

Note: \**p*-value calculated using Fisher's exact test.

Abbreviations: LN: Lymph node; PSA: Prostate-specific antigen.



nodes on MRI in 8/23 (34.8%) patients with nodal metastasis. Although 83.3% of patients with lymph node metastasis were  $\geq T2$ , this association was not statistically significant ( $p = 0.5$ ) and therefore cannot be considered meaningful.

The fundamental limitations of traditional imaging criteria may account for the comparatively poor diagnostic performance of MRI in predicting lymph node metastasis found in our investigation. To distinguish between benign and malignant nodes, MRI primarily relies on morphological characteristics, particularly lymph node size.<sup>29,30</sup> However, a number of studies have shown that a large percentage of metastatic lymph nodes in prostate cancer are small and fall within normal size ranges, which results in decreased sensitivity and under-detection.<sup>31</sup> Previous meta-analyses that reported MRI's poor sensitivity (about 39–42%)<sup>21</sup>, despite its relatively high specificity, mirrored this. Further reducing diagnostic accuracy is the possibility of false-positive results due to reactive or inflammatory lymph node enlargement.<sup>30</sup>

Recently, prostate-specific membrane antigen positron emission tomography (PSMA-PET), an emerging imaging modality, has demonstrated encouraging results in enhancing the detection of lymph node metastases in prostate cancer. Compared with traditional imaging modalities such as MRI, recent investigations have shown that PSMA-PET offers substantially greater sensitivity and overall diagnostic accuracy, particularly for detecting small or otherwise occult metastatic lymph nodes.<sup>32</sup> Furthermore, PSMA-based imaging addresses the main drawbacks of size-based imaging criteria by enabling the detection of disease beyond conventional anatomical bounds.<sup>33</sup> These results imply that preoperative staging and risk classification in patients with prostate cancer may be improved by combining sophisticated imaging modalities with traditional MRI.<sup>34</sup> Despite these developments, access to these imaging modalities remains restricted in many settings, underscoring the ongoing significance of assessing the diagnostic efficacy of traditional MRI methods.

The reference standard for nodal staging in prostate cancer is still histological examination after PLND; however, it also has limitations. Anatomical research has shown that the prostate's lymphatic drainage goes beyond traditional dissection templates.<sup>35</sup> Other pathways, such as the pararectal and presacral lymphatic routes, are infrequently used in surgical procedures and may lead to underestimation of nodal disease. Furthermore, the completeness of nodal sampling is further challenged by notable inter-individual anatomical variability in lymph node distribution.<sup>36</sup> Limitations in pathological processing

may lead to under-detection of lymph nodes, even when considerable dissection is performed. This is because a significant percentage of nodes may be missed by gross examination alone; up to 41.9% of nodes may only be found following thorough histological investigation.<sup>33</sup>

Although the limited diagnostic performance of MRI for lymph node staging is well established<sup>29</sup>, our findings provide additional insights into its performance in a real-world clinical setting with limited access to advanced imaging modalities such as PSMA-PET. Furthermore, this study highlights the discrepancy between statistical association and true predictive performance, emphasizing that statistically significant findings do not necessarily translate into clinically useful diagnostic tools.

Magnetic resonance imaging findings may warrant further investigation in combination with clinical variables in larger cohorts. The novelty of this study lies in the prospective evaluation of combined imaging and clinical parameters, particularly PSA density, in predicting lymph node metastasis. While MRI alone demonstrated limited utility, its combination with clinical markers may offer incremental value in risk stratification. The results of this study should be interpreted as exploratory, and its findings are intended to inform future larger-scale investigations rather than provide definitive conclusions.

## 5. Conclusion

Our data show that preoperative MRI findings have limited predictive value for pathologic lymph node metastasis when used alone. However, when it is combined with clinical parameters such as PSA density, the predictive power may improve. To properly evaluate the significance of preoperative MRI in detecting lymph node metastasis in prostate cancer, a large-scale, multicenter, prospective study is required.

This study has several limitations. The sample size was relatively small ( $n = 30$ ), with a limited number of patients demonstrating lymph node metastasis, which may affect statistical power and the stability of the findings. Additionally, the study was conducted at a single center, which may limit the generalizability of the results. Although MRI images were interpreted independently by two radiologists, inter-reader agreement was not formally assessed using statistical measures such as kappa analysis, which may introduce variability in imaging interpretation. Furthermore, multivariate analysis was not performed due to the limited sample size, restricting the ability to identify independent predictors. Finally, tumor size was not consistently reported in MRI assessments, preventing evaluation of its association with lymph node metastasis.

## Acknowledgments

None.

## Funding

None.

## Conflict of interest

The authors declare no conflict of interest.

## Author contributions

*Conceptualization:* Hardi Shwan Mahialdin

*Formal analysis:* Hana Rizgar Muhammed Ameen

*Investigation:* All authors

*Methodology:* Hardi Shwan Mahialdin

*Writing—original draft:* Hardi Shwan Mahialdin

*Writing—review & editing:* Hana Rizgar Muhammed Ameen

## Ethics approval and consent to participate

Ethical approval for this study was obtained from the Arab Board for Medical Specializations Ethics Committee. The research proposal was reviewed and approved on March 1, 2022, prior to the commencement of the study (Approval No: Not issued). The committee approved all aspects of the study, including patient recruitment, data collection, and analysis. In addition, institutional permission was obtained from Rizgary Teaching Hospital to conduct the study. All participants were adequately informed about the aims and procedures of the study, and written informed consent was obtained from each participant prior to inclusion. Participation was voluntary, and confidentiality of patient data was strictly maintained throughout the study.

## Consent for publication

Written informed consent was obtained from all participants for inclusion in the study. All data were anonymized, and no identifiable personal information or images are included in this manuscript.

## Availability of data

The data that support the findings of this study are available from the corresponding author upon reasonable request, subject to institutional and ethical approval.

## References

1. Ferlay J, Soerjomataram I, Dikshit R, *et al.* Cancer incidence and mortality worldwide: sources, methods and major patterns in GLOBOCAN 2012. *Int J Cancer.* 2015;136(5):E359-E386.  
doi: 10.1002/ijc.29210
2. Humphrey PA, Moch H, Cubilla AL, *et al.* The 2016 WHO classification of tumours of the urinary system and male genital organs—Part B: prostate and bladder tumours. *Eur Urol.* 2016;70(1):106-119.  
doi: 10.1016/j.eururo.2016.02.028
3. Rawla P. Epidemiology of prostate cancer. *World J Oncol.* 2019;10(2):63-89.  
doi: 10.14740/wjon1191
4. Barber L, Gerke T, Markt SC, *et al.* Family history of breast or prostate cancer and prostate cancer risk. *Clin Cancer Res.* 2018;24(23):5910-5917.  
doi: 10.1158/1078-0432.CCR-18-0370
5. Yatani R, Chigusa I, Akazaki K, Stemmermann GN, Welsh RA, Correa P. Geographic pathology of latent prostatic carcinoma. *Int J Cancer.* 1982;29(6):611-616.  
doi: 10.1002/ijc.2910290602
6. Mucci LA, Wilson KM, Giovannucci EL. Epidemiology of prostate cancer. In: *Pathology and Epidemiology of Cancer.* International Publishing: Springer; 2017:107-125.  
doi: 10.1007/978-3-319-35153-7\_9
7. Markozannes G, Tzoulaki I, Karli D, *et al.* Diet, body size, physical activity and risk of prostate cancer: an umbrella review of the evidence. *Eur J Cancer.* 2016;69:61-69.  
doi: 10.1016/j.ejca.2016.09.026
8. Li L, Wang L, Feng Z, *et al.* Prostate cancer magnetic resonance imaging (MRI): multidisciplinary standpoint. *Quant Imaging Med Surg.* 2013;3(2):100-112.  
doi: 10.3978/j.issn.2223-4292.2013.03.03
9. Hambrock T, Fütterer JJ, Huisman HJ, *et al.* Thirty-two-channel coil 3T magnetic resonance-guided biopsies of prostate tumor suspicious regions identified on multimodality 3T magnetic resonance imaging: technique and feasibility. *Invest Radiol.* 2008;43(10):686-694.  
doi: 10.1097/RLI.0b013e31817d0506
10. Tan CH, Wei W, Johnson V, Kundra V. Diffusion-weighted MRI in the detection of prostate cancer: meta-analysis. *AJR Am J Roentgenol.* 2012;199(4):822-829.  
doi: 10.2214/AJR.11.7805
11. Heijmink SW, Scheenen TW, Fütterer JJ, *et al.* Prostate and lymph node proton magnetic resonance (MR) spectroscopic imaging with external array coils at 3 T to detect recurrent prostate cancer after radiation therapy. *Invest Radiol.* 2007;42(6):420-427.  
doi: 10.1097/01.rli.0000262759.46364.50
12. Verma S, Turkbey B, Muradyan N, *et al.* Overview of dynamic contrast-enhanced MRI in prostate cancer diagnosis and management. *AJR Am J Roentgenol.* 2012;198(6):1277-1288.

- doi: 10.2214/AJR.12.8510
13. Montironi R, Cheng L, Cimadamore A, *et al.* Narrative review of prostate cancer grading systems: will the Gleason scores be replaced by the grade groups? *Transl Androl Urol.* 2021;10(3):1530-1540.  
doi: 10.21037/tau-20-853
  14. Chen N, Zhou Q. The evolving Gleason grading system. *Chin J Cancer Res.* 2016;28(1):58-64.  
doi: 10.3978/j.issn.1000-9604.2016.02.04
  15. Walsh PC. Radical prostatectomy for localized prostate cancer provides durable cancer control with excellent quality of life: a structured debate. *J Urol.* 2000;163(6):1802-1807.
  16. Cheng L, Zincke H, Blute ML, Bergstralh EJ, Scherer B, Bostwick DG. Risk of prostate carcinoma death in patients with lymph node metastasis. *Cancer.* 2001;91(1):66-73.  
doi: 10.1002/1097-0142(20010101)91:1<66::AID-CNCR9>3.0.CO;2-P
  17. Daneshmand S, Quek ML, Stein JP, *et al.* Prognosis of patients with lymph node positive prostate cancer following radical prostatectomy: long-term results. *J Urol.* 2004;172(6 Pt 1):2252-2255.  
doi: 10.1097/01.ju.0000143448.04161.cc
  18. Michalik B, Engels S, Kampmeier L, *et al.* Can contralateral lymph-node metastases be ruled out in prostate cancer patients with only unilaterally positive prostate biopsy? *Int J Clin Oncol.* 2023;28(12):1659-1666.  
doi: 10.1007/s10147-023-02407-w
  19. Roberts MJ, Yaxley JW, Stranne J, van Oort IM, Tilki D. Is extended pelvic lymph node dissection REALLY required for staging of prostate cancer in the PSMA-PET era? *Prostate Cancer Prostatic Dis.* 2025;28(2):345-347.  
doi: 10.1038/s41391-024-00821-3
  20. Fortuin A, de Rooij M, Zamecnik P, Haberkorn U, Barentsz J. Molecular and functional imaging for detection of lymph node metastases in prostate cancer. *Int J Mol Sci.* 2013;14(7):13842-13857.  
doi: 10.3390/ijms140713842
  21. Hövels AM, Heesakkers RA, Adang EM, *et al.* The diagnostic accuracy of CT and MRI in the staging of pelvic lymph nodes in patients with prostate cancer: a meta-analysis. *Clin Radiol.* 2008;63(4):387-395.  
doi: 10.1016/j.crad.2007.05.022
  22. Mottet N, Bellmunt J, Bolla M, *et al.* EAU-ESTRO-SIOG guidelines on prostate cancer. Part 1: screening, diagnosis, and local treatment with curative intent. *Eur Urol.* 2017;71(4):618-629.  
doi: 10.1016/j.eururo.2016.08.003
  23. Briganti A, Larcher A, Abdollah F, *et al.* Updated nomogram predicting lymph node invasion in patients with prostate cancer undergoing extended pelvic lymph node dissection: the essential importance of percentage of positive cores. *Eur Urol.* 2012;61(3):480-487.  
doi: 10.1016/j.eururo.2011.10.044
  24. Roach M, Marquez C, Yuo HS, *et al.* Predicting the risk of lymph node involvement using the pretreatment prostate-specific antigen and Gleason score in men with clinically localized prostate cancer. *Int J Radiat Oncol Biol Phys.* 1994;28(1):33-37.  
doi: 10.1016/0360-3016(94)90138-4
  25. Gandaglia G, Fossati N, Zaffuto E, *et al.* Development and internal validation of a novel model to identify candidates for extended pelvic lymph node dissection in prostate cancer. *Eur Urol.* 2017;72(4):632-640.  
doi: 10.1016/j.eururo.2017.03.049
  26. Abdollah F, Suardi N, Gallina A, *et al.* Extended pelvic lymph node dissection in prostate cancer: a 20-year audit in a single center. *Ann Oncol.* 2013;24(6):1459-1466.  
doi: 10.1093/annonc/mdt120
  27. Brembilla G, Dell'Oglio P, Stabile A, *et al.* Preoperative multiparametric MRI of the prostate for the prediction of lymph node metastases in prostate cancer patients treated with extended pelvic lymph node dissection. *Eur Radiol.* 2018;28(5):1969-1976.  
doi: 10.1007/s00330-017-5229-6
  28. Ryu H, Song B, Hwang J, *et al.* Pelvic lymph node metastases in prostate cancer: preoperative detection with dynamic contrast-enhanced magnetic resonance imaging compared with postoperative pathologic result of pelvic lymph node dissection. *Korean J Urol Oncol.* 2017;15(3):158-164.  
doi: 10.22465/kjuo.2017.15.3.158
  29. Zarzour JG, Galgano S, McConathy J, Thomas JV, Rais-Bahrami S. Lymph node imaging in initial staging of prostate cancer: an overview and update. *World J Radiol.* 2017;9(10):389-399.  
doi: 10.4329/wjr.v9.i10.389
  30. Pasoglou V, Michoux N, Tombal B, Lecouvet F. Optimising TNM staging of patients with prostate cancer using WB-MRI. *J Belg Soc Radiol.* 2016;100(1):101.  
doi: 10.5334/jbr-btr.1209
  31. Daouacher G, Waldén M, Carlsson J, *et al.* Diagnostic performance of conventional MRI using T1W and T2W for primary lymph node staging in intermediate- and high-risk prostate cancer patients prior to pelvic lymph node dissection. *Abdom Radiol.* 2025;51(1):206-213.  
doi: 10.1007/s00261-025-05073-w
  32. Yang B, Dong H, Zhang S, *et al.* PSMA PET vs mpMRI for lymph node metastasis of prostate cancer: a systematic

- review and head-to-head comparative meta-analysis. *Acad Radiol.* 2025;32(5):2797-2814.  
doi: 10.1016/j.acra.2024.11.029
33. Wang X, Wen Q, Zhang H, Ji B. Head-to-head comparison of 68Ga-PSMA-11 PET/CT and multiparametric MRI for pelvic lymph node staging prior to radical prostatectomy in patients with intermediate- to high-risk prostate cancer: a meta-analysis. *Front Oncol.* 2021;11:737989.  
doi: 10.3389/fonc.2021.737989
34. Mazzone E, Cannoletta D, Quarta L, *et al.* A comprehensive systematic review and meta-analysis of the role of prostate-specific membrane antigen positron emission tomography for prostate cancer diagnosis and primary staging before definitive treatment. *Eur Urol.* 2025;87(6):654-671.  
doi: 10.1016/j.eururo.2025.03.003
35. Boscolo-Berto R, Siracusano S, Porzionato A, *et al.* The underestimated posterior lymphatic drainage of the prostate: an historical overview and preliminary anatomical study on cadaver. *Prostate.* 2019;80(2):153-161.  
doi: 10.1002/pros.23927
36. Tunksakul P, Piyaman P, Woranisarakul V, *et al.* Cadaveric evidence on lymph node counts and grossing accuracy in pelvic lymph node dissection for prostate cancer staging. *Sci Rep.* 2025;16(1):120.  
doi: 10.1038/s41598-025-29196-8